**Ministry of Higher Education
and Scientific Research**

Journal of Kufa for Chemical Sciences

A refereed

Research Journal Chemical Sciences
Vol.2 No.8 Year 2022
ISSN 2077-2351

Address:
Iraq-Najaf-University of Kufa
Box(190)

www.Edu_girl.Kuiraq.com

E-mail:Edu_grils@kuiraq.com

Thermodynamic and Kinetic Study for Removal of MB and CR from Aqueous Solution Using of SD and SD/MgO -Nanoparticles as Biosorbents

Awaz A. Taher and Rounak M. Shariff

Department of Chemistry College of Science, University of Salahaddin-Erbil,
Kurdistan Region, Iraq
rounak.shariff@su.edu.krd

الملخص

دراسة ديناميكية حرارية لفحص المادة المازة الحيوية من أشجار الصنوبر ونشارة الخشب (SD) ونشارة الخشب المكسوة بأكسيد المغنيسيوم (MgO) والجسيمات النانوية (SD/MgO) لإزالة الصبغات الكاتيونية (الميثيل الأزرق ، MB) والأنيونية (الكونغو الأحمر CR) في تقنية الامتزاز غيرالمستمرة (دفعات) . خلال هذه الدراسة تم إجراء توصيفات لكل مادة مازة بواسطة FTIR و SEM و XDR. متغيرات مختلفة لتجارب توازن الدُفعات التي تم تشكيلها مسبقًا لفحص التقارب لعملية الامتزاز لكل صبغة على كل مادة مازة. تُستخدم نتائج البيانات في دراسة الخواص الحركية لتتلاءم مع قانون الرتبة الزائفة من الدرجة الأولى وقانون معدل الرتبة الثانية الزائفة وقانون الانتشار داخل الجسيمات. تم تطبيق Freundlich و Langmuir و Temkin كنماذج متساوية الحرارة لوصف تقارب الامتزاز. كشفت البيانات أن MB و CR صبغات الممتزة على سطح SD و SD / MgO كانت متطابقة مع الترتيب الثاني الزائف و Freundlich. تفاوتت قيم K_F لامتزاز الأصباغ MB و CR على SD و SD/MgO بين (67.19-31.88) و (44.05 - 46.63) و (276.3864.6) و (57.74 - 170.69) mlg^{-1} ، بينما اختلفت قيم K_L بين (0.004-0.008) و (0.008- 0.012) و (0.005-0.012) و (0.032-0.009) mlg^{-1} عند درجات الحرارة المختلفة على التوالي. تم حساب قيم المعامل الديناميكية الحرارية (ΔG^o، ΔH^o، ΔS^o) عند 25 ، 35 ، 45 ± 1 درجة مئوية. القيم السالبة لـ ΔG^o تعني أن عمليات الامتزاز لها طبيعة ماصة للحرارة و تلقائية و يفضل في الدرجات الحرارية العالية. والتي أثبتتها القيمة الإيجابية لـ ΔH^o التي تتحكم في الامتزاز الكيميائي على الرغم من زيادة درجة الحرارة ، بينما العشوائية على سطح الامتزاز على سطح الممتزات بسبب القيم الموجبة من ΔS^o.

Abstract

Thermodynamic study for investigation of the biosorbent from Pine trees, sawdust (SD) and sawdust veneered with magnesium oxide (MgO), (SD/MgO) Nanoparticles for removal of Cationic (Methyl blue, MB) and anionic (Congo Red CR) dyes in a batch process. Characterizations for each biosorbents were done by FTIR, SEM, and XDR. Various parameters for batch equilibrium experiments preformed to examine the affinities for adsorption process for each dyes on each adsorbents. The data results in the kinetics study are used to fit with the Pseudo-first order and Pseudo-second order rate law, and intra particle diffusion models. The Freundlich, Langmuir, and Temkin, were applied as isothermal models to describe the adsorption convergence. The Data revealed that MB and CR dyes adsorption onto SD and SD/MgO has a good agreement with pseudo-second order and Freundlich. The K_F values for MB and CR dyes adsorption onto SD and SD/MgO varied between [31.88-67.19, 44.05-46.63, 276.3-864.6, and 57.74-170.69]mlg^{-1}, while K_L values varied between [0.008-0.004, 0.012 -0.008, 0.012-0.005, and 0.009-0.032]mlg^{-1} at the three temperatures respectively. The values of thermodynamic parameters (ΔG, ΔH, ΔS) were calculated at 25, 35, 45 ±1ºC. The negative values for ΔG means that the adsorption processes spontaneous and has endothermic nature which proved by the positive value of ΔH that control the chemisorption adsorption in spite of increasing temperature, while the randomness at the surface of the adsorabt on the adsorbent surface due to the positive of the ΔS.

1. Introduction

Non-biodegradable and polluting nature of the colorants materials and dyes constitute is an environmental hazard through its contamination to underground water as a final step [1, 2].The feature of the Azo dyes class which have variety in structural and color, they form aromatic amines as an eventually reduces linkage[3]. As the dyes binding to natural textile fibers, leather, paper, plastic, mineral oils relocate to environmental [4]. Methyl blue (MB) classified as basic or cationic dyes which are more toxic than anionic dyes[5]. MB cause eye burns for human and animals its hazardous description, it cause nausea and difficulty in breath on inhalation [6].The removing of MB has been important from the waste water. Congo red (CR) Classified as anionic secondary diazo dye, it contains azo (-N=N-) chromophore and an

acidic (-SO_3H), or acidic diazo dye, it has a carcinogenicity cause [7&8], it resist biodegradation, it has been used in many industries [9].

Chemical and physical methods can be used including adsorption which is one of the most significant for the removal of the days [10&11]. Many technical processes have been applied for the removal of the dyes from waste water [12&13]. The adsorption processes is effective key for determination and choosing the adsorbent which possess high capacity, low coast and cheap [14&15]. The development of the adsorbents from waste material and cheap such as: peat[16], Activated Carbon [17], Rise husk [18], Cotton waste [19], Clay [20], Sawdust [21].

In this work we use the sawdust as a waste material from Pine trees for the removal of MB and CR by batch process from aqueous solutions. The powerful of SD coated with magnesium oxide and forming nanoparticle of SD/MgO increases the active site for adsorption [22]. The values of thermodynamic parameters such as Gibbs free energy (ΔG^o), heat of adsorption (ΔH^o), entropy change (ΔS^o) and activation energy (Ea^o) for adsorption also studied, which it affirm the nature of the process if its endothermic or exothermic [23].

2. Materials and Experimental Methods

2.1. Adsorbate

Methylene blue MB [3,7-bis (dimethylamino)-phenthiazineium-5-chloride] is a basic cationic dye the structure shown in Figure1. a, its molecular formula: $C_{16}H_{18}ClN_3S.\ 3H_2O$, Molecular weight 327.22 g mol^{-1}, and the analysis wavelength (λ_{max}) 664 nm.

Congo red CR [1- Naphthalenesulfonic acid, 3,3’ – [(1,1’ – biphenyl) – 4,4’ –diylbis(2,1 –dizenediyl)] bis [4-amino-,sodium salt (1:2)], is an acidic, anionic diazo dye, and aromatic water soluble dye, the structure shown in Figure1.b,its molecular formula: $C_{32}H_{22}N_6Na_2O_6S_2$, Molecular weight 696.66 g mol^{-1}, analysis wavelength (λ_{max}) 500 nm.

A stock solution for each dye alone were prepared (100mg/L) by dissolving required amount of dye in deionized water to obtain desired concentration ranging from 1 to100 mgL^{-1}. The two are from (BDH chemicals Ltd pool England). The concentration of the dye in the experimental solution was determine from calibration curve prepared by measuring absorbance of different determined concentration of MB and CR alone at using UV-vis Spectrophotometer (Model

CeCIL, Ce 3021, 3000 series) [24 &25]. Figure 2. demonstrated the λ_{max} value of (A) BM and (B) CR dyes.

2.2. Adsorbent

The adsorbent used in the present study was collected from selected local Pine tree, the sawdust as a waste material from Pine tree. These natural wastes washed and rinsed very well with tap water to remove the soil, dust and soluble material then air-dried at room temperature which was about 50°C for two weeks [26&27]. The dried sample was grounded to a fine powder in a still mill. The resulted material was sieved with sieve set containing 30-250 µm mesh sieve, and storage it in an airtight plastic container and used for analysis as well as for adsorption experiments without any pre-treatment.

The moisture content measurement done by, 2g of adsorbent dried in an oven at temperature 103°C and then the rest stored in the bottle to use. In adsorption experiment a certain amount of adsorbent was added to a certain amount of dye solution [28]. The PH of solution powder for each type was measured by pH meter (EUTECH instrument CON 510, Conductivity, TDS meter) shown in Table 1. The powder for each type was analyzed by the Spectrum FTIR spectrometer to determined functional groups as shown in Figure 3. a. Figure 4. Shows the XRD diffractogram, the diffraction was done by scanning on (Philips PW3050 Cu radiation in Iran Republic) in range 0-70 ^{o} (2θ). Figure 5. Demonstrated the SEM micrographs for SD, the images captured by a Mira 3-XMU (TESCAN, in Iran Republic)

2.2.1 Adsorbent by further modification.

The SD/MgO adsorbent preparation and modification don by 10 g of grounded powder of SD treated with 0.3M Magnesium sulfate heptahydrate ($MgSO_4.7H_2O$) and then, till the precipitation appeared and completed adding drowsily NaOH to the mixture under stirring at room temperature. Then washed with distilled water and filtered then dried in an oven at 90°C for 6h. The modified product is nanoparticles MgO veneered on the selected adsorbent prepared. The conversion of Magnesium hydroxide deposited and formed by the reaction to Magnesium oxide as a result of heating [29]. Table 1. Shows the analyzes for moister which is zero, pH, CEC and TDS. While the Spectrum of FTIR spectrometer shown in Figure 3. a., Figure4. XRD diffractogram and Figure 5., SEM micrographs for SD/MgO.

2.3. Batch Adsorption Experiments

2.3. 1. Optimization Conditions of Adsorption

Batch adsorption of the each dyes MB and CR alone from aqueous solution was determined at temperature (25±1 C˚) employing optimum standard batch equilibrium method. The effect of the of initial dye concentration, contact time, solution temperature, and solution pH on the adsorption uptake the adsorption of MB and CR dyes each alone onto each SD and SD/MgO were studied alone. Adsorption isotherm was accomplished by putting 10 ml of dye with deferent initial concentration (10-150) mgl^{-1} in a set of 18 ml tube fitted with Teflon–lined screw caps. Equal amount of adsorbent of 400mg of particle size (250µm) for SD, and 100mg of SD/MgO were added to the dye solutions [6&7]. Each adsorbent samples were equilibrated with different MB and CR dye concentrations (10, 25, 50, 75, and 100 µg ml^{-1}) for duplicate. Another two sets of this solid-solution mixture prepared once without dye used as blank, and the other without adsorbent used as control were and placed in shaker for 30, 60, 120, 180, 240, 300 min. The solid-solution mixtures were centrifuged for 30 min. at 3500 rpm. The pH of dye solution was adjusted to (6) by using 0.1N NaOH and 0.1 N HCl. The experiments sample solutions were withdrawn at intervals to determine the residual concentration by using UV-Vis spectrophotometer at 664 and 500 nm wavelengths for MB and CR respectively.

To study the effect of temperature the same experiments done at temperature (25, 35, 45 ±1 C˚) employing a standard batch equilibrium method[9]. Different temperature were investigated on color dyes removal at (10, 25, 50, 75, and 100) µg ml^{-1} concentration of dyes MB and CR by SD and SD/MgO, dosage of 400 and 100 mg respectively.

$$q_e = (C_o - C_e)\frac{V}{W} \qquad (1)$$

$$q_t = (C_o - C_t)\frac{V}{W} \qquad (2)$$

$$Dye\,\mathrm{Re}\,moval\% = \frac{C_o - C_e}{C_o} x100 \qquad (3)$$

q_e (mg g^{-1}) represents the capacity of the equilibrium adsorption C_o and C_e are initial and equilibrium dye concentration (mg L^{-1}), respectively. V is the volume of the solution (L) and W is the dry weight of the adsorbent (g). While the value of adsorption at time t q_t

(mg g^{-1}). In order to get values from the samples, the measuring from all of the samples was taken in triplicates and then the mean values were calculated and were used for further analysis. The equations above were used to determine the capacity of the equilibrium adsorption and removal %.

2.3.2 Fourier Transform Infrared Spectra

Fourier Transform Infrared Spectrophotometer FTIR was important to identify the functional groups that were responsible for adsorbing pollutant ions. The SD (10mg) was ground with 200mg KBr (spectroscopic grade) in a mortar pressed into 10mm diameter disks less than 10 tons of pressure and high vacuum for 10 min. The Fourier Transform Infrared Spectrophotometer FTIR spectra were obtained on a Shimadzu corporation kyoto Japan, model IR Affinity-1 spectrometer.

The FTIR spectra before adsorption and after sorption of MB and CR were used to determine the vibrational frequency changes in the functional groups present in the adsorbent. The spectra of adsorbents were measured within the range from 600-4000 cm^{-1} wave number. The spectra were plotted using the same scale on the transmittance axis for all the adsorbent before and after adsorption. Figure3. and Table 2. shows the tabulated data for FTIR spectra band assignments for samples. These spectral lines describe the various changes that observed through the adsorption process when some peaks were shifted or disappeared and the new peaks are also detected in the samples. The spectra display a number of absorption peaks, reflecting the complex nature of the adsorbent [30].

3. Data analysis

3.1. Adsorption Kinetics

The possible mechanism that was suitable to explain the adsorption process is kinetic study which is related to the equilibrium time. Using pseudo-first order, and pseudo-second order using equation 4 and 5 expressed as below; The rate constants for adsorption of each dyes on each adsorbents were calculated using the rate expression [31,32]:

$$\log(q_e - q_t) = \log q_e - \frac{k_1}{2.303} t \qquad (4)$$

$$\frac{t}{q_t} = \frac{1}{k_2 q_e^{\,2}} + \frac{t}{q_e} \qquad (5)$$

Where: K_1, and K_2 are the rate constant for pseudo-first order adsorption (min^{-1}), pseudo-second order adsorption (g/mg min) respectively. The t is time (min). The data by linear plots as shown in (Table 3, 4, and 5), also Figures 10 and 11 for applying pseudo-second order for adsorption of MB, and CR dye by using SD/MgO nano-biocomposite at different temperature.

Intra-particle diffusion [33, 34] expressed in equation in (6), and the K_{id} is the rat constant (mg/ (g min ^{½}).

$$q_t = k_{id}\sqrt{t} + C \qquad (6)$$

Where k_p is rate constant stands for the intra-particle diffusion (mg g^{-1}). C is the intercept (mg g^{-1}) the boundary layer's thickness, so the plots of q_t versus t which describes as rate controlling step. The data demonstrated in Table 3, 4, and 5.

3.2. Adsorption Isotherms

The Frendlich model as expressed in the equation below which assumes that layer after layer of dyes molecules adsorb on the adsorbent surface. Adsorption isotherm parameters were calculated using the linearized form of Freundlich equation [35, 36]:

$$\ln q_e = \ln K_F + \frac{1}{n}\ln C_e \qquad (7)$$

K_F is Freundlich adsorption constant related to the capacity of adsorption (µg g^{-1}), and n is the intensity of adsorption. The values of K_F, n, and the regression equation showed (Table 6, 7, and 8).

The Langmuir model as expressed in the equation below. Data from the batch adsorption conform to Langmuir equation [37, &38]:

$$q_e = \frac{q_e K_L C_e}{1 + K_L C_e} \qquad (8)$$

q_o is the monolayer capacity of the adsorbent (mg g^{-1}) and q_e is the adsorption constant (mg ml^{-1}). The results were summarized in (Table 6, 7, and 8), and Figures 12, and 13.

Equation 6 express the model of R Temkin[39]. The results were summarized in (Table 6, 7, and 8).

$$q_e = B\,(\ln A + \ln C_e) \qquad (9)$$

The correlation coefficients R^2 value and normalized standard deviation Δ q_e were the two important factor for concluding the pertinence and suitability of the isotherm equations. Figures 12, and 13 for adsorption Isotherm models for Freundlich, Langmuir and Temkine for MB & CR on SD & SD/Mgo at different temperatures.

3.3. *Thermodynamic parameters*

The activation energy for the adsorption of selected dyes onto prepared adsorbents was evaluated using the following form of Arrhenius equation [40].

$$LnK_o = \ln A - \frac{E_a}{RT} \qquad (10)$$

The equilibrium constant (K_o) was enabled us to calculate the thermodynamic parameters for physico-chemical equilibrium, the thermodynamic parameters associated with adsorption process were calculated from the variation of the thermodynamic equilibrium constant (K_o), Values of $\ln K_o$ are obtained from the plot of ln (C_s/C_e) vs. C_s, the $\ln K_o$ was obtained at C_s = 0. Values of $\ln K_o$ were in the range 1.238 - 16.17 $KJmol^{-1}$. The activation for the adsorption and the Arrhenius factor were calculated from the plot of the ln k_o Vs 1/T. The thermodynamic parameters were evaluated using the following mathematical relationship. The standard free energy change values of constant K_o, can be expressed in terms of the standard Gibbs or free energy for adsorption (ΔG) [41]**.** The results were summarized in table 9.

$$\Delta G^o = -RTLnK_o \qquad (11)$$

The standard enthalpy change of adsorption **(**ΔH^o), and standard entropy change **(**ΔS^o) were determined graphically from the following equation[41]:

$$LnK_o = \frac{\Delta S^o}{R} - \frac{\Delta H^o}{RT} \qquad (12)$$

Plotting $-LnK_o$ against 1/T, a straight line is expected the ΔH^o and ΔS^o of were determined from the slope and intercept as shown in Fig14**.** The results were summarized in table 9.

4. Results and Discussion

4.1. Characterization of SD and SD/MgO

The adsorption capacity of SD depends on porosity and reactivity of functional groups at the surface. The FTIR spectrum in figure- 3 - shows that OH and NH stretching is between 3100 – 3500 cm^{-1} , C-H aromatic is between 3000 – 3100 cm^{-1} , and C-H aliphatic is between 2800 – 3000 cm^{-1}. The spectrum shows a broad band near 3410.15 cm^{-1} which indicates the presence of hydroxyl groups on the SD surface [42&43]. The stretching was attributed to the absorbance water on the surface of SD. The peak at 2926.01cm^{-1} is due to C–H starching of CH_2 groups. The stretching frequencies of the aromatic C=C and aromatic C–H groups give rise to peaks at 3011 -2854cm^{-1} respectively. The bands near 1658.78 cm^{-1} indicates fingerprint region of C=O, C-O and O-H groups that exist as functional of SD [44]. The peaks at 1510.26 cm^{-1} is assigned to a conjugated hydrogen bonded carboxyl group. The peak at 1371.39 cm^{-1} indicates the presence of C–H aliphatic bending. The peak at 1373.32 cm^{-1} indicates the presence of C-N from amine. The two peaks at 1161.15 cm^{-1} (S=O) and 1058.92 cm^{-1} (S–OH) was characteristic of SO_2 stretching. These results agree with the surface chemistries of other agricultural by – products[45].

The O-H Group which appears as (phenols, carboxylic acids, and alcohols) as it's in cellulose as pectin and lignin in the region 3381.21 cm^{-1} [46]. The aliphatic C-H asymmetric stretching presence's in the region 2900.94 cm^{-1} . The C=O stretching vibration of carboxylic acid appears in 1730.15 cm^{-1} .The aromatic C=C stretching of lignin presence's in the region 1510.26 cm^{-1}. The C-O stretching vibration for carboxylic acids appears in 1269.16 cm^{-1}, while the C-H binding vibration appears in 896.90 cm^{-1}. Changes occur on spectrum after MB adsorption the intensity of the peaks decreased and shifted due to the interaction between them. The presence of some functional groups in SD/MgO nanoparticles as biosorbents which have a great roil in MB adsorption such as O-H, C=O, and C-O, and some new as N-H aromatic and S=O stretching [47].

The -COOH the intensities for the bands in the region 1600 cm^{-1} and 1731 cm^{-1}. The OH-group presence's in the region 3100 cm^{-1} and 3400 cm^{-1}. The C=O stretching vibration of carboxylic acid appears in 1730.15 cm^{-1} .The aromatic C=C stretching of lignin presence's in the region 1602.37 cm^{-1}. The C-O stretching vibration for carboxylic acids appears in1269.16 cm^{-1}, while the -CH_2 binding vibration appears in

1263.56 cm^{-1}. The -CH vibration appears in 2928.33 cm^{-1} The C-N stretching with amine 1263.56 cm^{-1} , aromatic and S=O stretching[48] .

The amorphously X-ray diffraction (XRD) analysis for each SD and SD/MgO nanoparticles as biosorbent, the peaks emerge at $2\theta = 38^{o}$ peak. The full width at half maximum (FWHM) which apply the Debye-Schherre formula, while the expected size about 5.2 nm, Figure 4. expose it [49].

Scanning Electron Microscopy (FE-SEM), distinct the surface images for SD, and SD/MgO nanoparticles as biosorbents. Figure 5. reveals that high surface area are available from both adsorbents which would be able to adsorb more component [50].

4.2. Effect of the other Factor's.

The effect of contact time on the removal of MB and CR by SD and SD/MgO at (10, 25, 50,and 75 µg 100 ml^{-1}) initial dye concentration with a SD dosage of 400 mg, and 100mg SD and SD/MgO respectively as shown in Figure 6. The removal of dye initially increases with time intervals as the amount of dye adsorbed. Indicated that adsorption is mostly dependent on the initial concentration of dyes.

The amount of adsorbent dosage affected on the dye removal. Various dosage (10 – 600) mg for each adsorbent used at dye concentration (10, 25, 50, and 75) μgml^{-1} were shown in Figure 7. As the dosage increased the removal of dye increased, as the more sit increased, the color changes prove this.

The pH solution change in the range of the (3-11) which effect on the adsorption of 100 µg ml^{-1} concentration of dyes (MB and CR) by SD and SD/MgO dosage of 400 and 100 mg respectively. The result presented in Figure 8. Increasing the pH meant increasing the appearance of negatively charged group on the adsorbent surface sites which been available for basic dyes adsorption. Figure 9, demonstrated the effect of concentration of dyes at $25^{o}C$ for (a) MB on SD and SD/MgO for MB, (b) CR on SD and SD/MgO.

The values of rate constant for the adsorption of MB and CR shown in Tables 3,4, and 5 on each SD and SD/MgO using three models first, second order rat law and power function equations; the values were in the range from 0.022 to 0.026 min^{-1} and 0.020 to 0.022 min^{-1} 0.023 to

0.029 min^{-1} 0.016 to 0.029 min^{-1} for MB and CR on SD and SD/MgO respectively for pseudo first order equations rat different temperature, while the value of regression factor R^2 from 0.714 to 0.999. For applying pseudo second order equations the data ranging from 0.002 to 0.004, 0.003 to 0.004, 0.001 to 0.011, and 0.001 to 0.008g $\mu g^{-1} min^{-1}$ for MB and CR on SD and SD/MgO respectively, while the value of regression factor R^2 from 0.824 to 0.999. The value of K_{id} (mg/ (g $min^{½}$) for Intra particle diffusion equation were from to; 0.088 to 0.761, 0.121to 1.088, 0.053 to 0.318, 0.045 to 398 for MB and CR on SD and SD/MgO respectively, while the value of regression factor R^2 from 0.716 to 0.999. The MB and CR exhibited the highe rate of accumulation with 59.1, 59.7, 75.3, 73.5 % adsorption on the SD and SD/MgO respectively after 60 min.

The effective isotherm models were: Freundlich adsorption describes for MB and CR on SD and SD/MgO as shown in Figures 12 and 13, values of K_F were varied from 31.9 – 67.19, 44.05- 46.62, 276.3-864.6 , 57.74- 170.7 mlg^{-1} respectively. The values of n all n>1 the variable slopes of the adsorption isotherm obtained for different systems studied reveal that the adsorption is complex phenomena involving different types of adsorption sites with different surface energies[36], while the value of regression factor R^2 from 0.873 to 0.999. The standard error S.E. values for MB, and CR on SD, and SD/MgO between 0.881– 0.999, 0.835-0.989, 0.139– 0.997, and 0.107-0.993 respectively. The regression equations relating that the highest values are the most fitted model, our results agreed with research [13].

Langmuir adsorption model describes isotherm for MB and CR on SD and SD/MgO as shown in Figures 12 and 13, with regression factor R^2 ranged between 0.996- 0.749, 0.749-0.829 , 0.945-0.889, 0.856-0.837 respectively, while the values of K_L ranged from 0.008- 0.004, 0.012-0.007, 0.012-0.005, 0.009-0.032 mlg^{-1} respectively. The maximum amount of for MB and CR on SD and SD/MgO adsorption (C_m) ranged from 2500 to 10000 mg g^{-1} the high C_m values on the examined could be explained by the high affinity [38]. The standard error S.E. values for MB, and CR on SD and SD/MgO between 0.201–0.140, 0.207-0.164, 0.133-0.198 and 0.140-0.969 respectively. The regression equations relating that the highest values are the most fitted model, our results agreed with research [13].

Temkin adsorption model describes isotherm for MB and CR on SD and SD/MgO as shown in Figures 12 and 13, with regression factor R^2

ranged between 0.963- 0.927, 0.908-0.939 , 0.949-0.928, 0.890-0.934 respectively, and the values of α ranged from 6.964-28.33, 8.63-33.86, 34.29-138, 33.21-36.61lg^{-1} respectively. The Value of β for MB and CR on SD and SD/MgO adsorption ranged between 516–499, 485-473, 2518-2644 and 2669-2524 Jmg^{-1} respectively , concluding that the two value α and β were the relation appropriate with the isotherm equations [39].

Data in Table 9 shows the effect of temperature on the adsorption dyes removal for MB and CR by SD and SD/MgO. The rate of diffusion of adsorbate molecules through adsorbent pores and, the boundary layer increased by increasing the temperature. Free energy change ΔG, standard entropy change ΔS and standard enthalpy change ΔH for adsorption of MB and CR on the SD and SD/MgO at three temperatures where obtained from the plot of 1/T vs lnk (Figure 14.). The adsorption is chemisorption due to ΔG value is between (0 to -20) KJ/mole[51] physisorption and (- 80 to – 400) its chemisorption. The negative value of ΔG and decreased with the rise in temperature, indicating that at all experimental temperatures; the interactions were spontaneous. The ΔG values were in the range -14.794 to -21.222, -14.853 to -19.618, -22.536 to -27.194, and -21.322 to 27.145 $KJmol^{-1}$. The adsorption processes has endothermic nature which proved by the positive value of ΔH that control the chemisorption adsorption in spite of increasing temperature. The values of enthalpy change ΔH followed the range 28.104 to 76.576 $KJmol^{-1}$. The randomness at the surface of the adsorabt on the adsorbent surface due to the positive of the ΔS, the values of entropy change ΔS followed the range 0.175-0.306 $Jmol^{-1}$ k^{-1}. The values of E_a for MB and CR dyes adsorption onto SD and SD/MgO(79.06,54.36, 30.75 and 50.46) kJ/mol respectively. The values of R^2 were in the range 0.823 to 0.927.

5. Conclusion

The biosorbents SD and SD/MgO coated with nanoparticles used for the removal of MB and CR from water solution. Kinetics experiments from batch process were used to investigate the behavior of each dye on each adsorbent. The adsorption of dyes increased with contact time, temperature and adsorbent dose. Optimization of pH of the adsorbent was found to be around 7. The correlation factor R^2 for Freundlich adsorption isotherm indicated that at high temperature chemisorption adsorption of CR and MB dyes on each biosorbents, while the adsorption was physisorption at low temperature. Adsorption experiments were conducted at 25, 35, and 45^oC to study

the thermodynamic parameter, associated with the adsorption of the studied each dyes on the each biosorbents. The MB dye molecules diffuse faster than CR molecules resulting in better removal of MB.

6. References

1. Crini,G., [2006]: Non-conventional low-cost adsorbents for dye removal: A review. Bioresource Technology. 97 (9), p.1061-1085.
2. Downham A., Collins P. [2000]: Coloring our foods in the last and next millennium. International Journal of Food Science and Technology. 35, p. 5-22.
3. C. Cripps, J.A. Bumpus, S.D. Aust, [1990]: Biodegradation of azo and heterocyclic dyes by phanerochaete chrysosporium, Appl. Environ. Microbiol. 56(4), p.1114-1118.
4. D. T. Sponza, M. Isik, [2005]: Toxicity and intermediates of C. I. Direct Red 28 dye through sequential anaerobic/ aerobic treatment, Process Biochem. 40, p.2735-2744.
5. Hao, J. O., Kim, H.m, and Chiang, P. C.[2000]: Decolourization of wastewater. Critical Reviews in Environmental Science and Technology. 30, p.449-505.
6. Abd El-Latif, M. M., Ibrahim, A. M., and El-Kady, M. F.[2010]: Adsorption equilibrium, kinetics and thermodynamics of methylene blue from aqueous solutions using biopolymer oak sawdust composite. J. Am. Sci. 6(6), p. 267-283.
7. R. Han, D. Ding, Y. Xu, W. Zou, Y. Wang, Y. Li, L Zou, [2008]: Use of rice husk for the adsorption of Congo red from aqueous solution in column mode, Bioressource Technol. 99, p. 2938-2946.
8. A. S. Raymundo, R. Zanarotto, M. Belisario, M. G. Pereira, J. N. Ribeiro, A. V. F. N. Riberio.[2010]: Evaluation of sugar-cane bagasse as bioadsorbent in the textile wastewater treatment contaminated with carcinogenic congo red dye, Brazilian Arch. Biology Technol. 53(4), p. 931-938.
9. V. Vimonses, S. Lei, B. Jin, C. W. K. Chow, C. Saint, [2009]: Kinetic study and equilibrium isotherm analysis of Congo Red adsorption by clay materials, Chem. Eng. J. 148, p. 354-364.
10. Robinson, T. McMullan, G. Marchant, R. Nigam, P.,[2001]: Remediation of dyes in textile effluent: A critical review on current treatment technologies with a proposed alternative. Bioresource Technology. 77 (3), p. 24-255.
11. Mavros P., Daniilidou A. C., Lazaridis N. K., Stergiou L.,[1994]: Color removal from aqueous-solution. I. Flotation. Environmental Technology. 15, p.601-616.

12. Yao, Z. L., Wang, J., and Qi. [2009]: Biosorption of methylene blue from aqueous solution using a bioenergy forest waste: Xanthoceras sorbifolia seed coat. Clean. 37(8), p. 642-648.
13. Karcher. S., Kornmuller, A. JekeL, M. [2002]: Anion exchange resins for removal of reactive dyes from textile wastewaters. Water Research. 36 (19), p. 4717-4724.
14. Saratale RG, Saratale GD, Chang JS, Govindwar SP. [2011]: Bacterial decolorization and degradation of azo dyes: a review. J Tawiwan Inst Chem Eng. 42, p. 138-57.
15. Gupta V.K., Gupta B, Rastogi A, Agraewal S, Nayak A. [2011]: A comparative investigation on adsorption performances of mezoporous activated carbon prepred from waste rubber tire and activated carbon for hazardous azo dye- acid blue 113. J Hazard Mater. 186, p. 891-901.
16. Allen S.J., Mckay G. and Porter J.F. [2004]: Adsorption isotherm models for basic dye adsorption by peat in single and binary component systems, Journal of Colloid and interface Science. 280, p. 322-333.
17. Rodriguez A., Garcia J., Ovejero G. and Mestanza M. [2009]: Adsorption of anionic and cationic dyes on activated carbon from aqueous solution: Equilibrium and kinetics, Journal of Hazardous Materials. 172, p.1311-1320.
18. Vadivelan, V., Kumar, K. V. [2011]: Equilibrium, kinetics, mechanism and process design for the sorption of methylene blue onto rice husk. Journal of Colloid and Interface Science. 286, p. 90-100.
19. Deng, H., Lu, J. Li., G., Zhang, G., Wang, X. [2011]: Adsorption of methylene on adsorbent matrials produced from cotton stalk. Chemical Engineering Journal. 172 (1), p. 326-334.
20. Hajjaji M., Alami A., El Bouadili A. [2006]: Removal of methylene blue from aqueous solution by fibrous clay minerals. Journal of Hazardous Materials. B135, p. 188-192.
21. Garg, V. K., Gupta, R., Yadav, A. B. and Kumar, R.[2003]: Rye removal from aqueous solution by adsorption on treated sawdust, Bioresource Technology. 89, p. 121-129.
22. Garg, V. K., Amita, M., Kumar, R. and Gupta, R. [2004]: Basic dye (methylene blue) removal from simulated wastewater by adsorption using Indian rosewood sawdust: A timber industry waste. Dyes and pigments. 63, p. 243-250.
23. M. K. Purkait, Maiti, S. D.S.Gupta, S. De, [2007]: Removal of Congo Red using activated carbon and its regeneration, J. Hazard. Mater. 145, p. 287-295.

24. Tusliar Kauti Sen. Slinrmeen Afroze-H Aug. [2011]: Equilibrium, Kinetics and Mechanism of Removal of Methylene Blue from Aqueous Solution by Adsorption onto Pine Cone Biomass of Pinus radium. Water Air Soil Pollut. 218, p. 499-515.
25. S Kalai Selvil and N Suganthi. [2017]: Removal of Anionic and Cationic Dyes from Aqueous Solution by Phosphoric Acid Modified Eichhornia Crassipes: Regeneration. 6 (24), p. 2541-2557.
26. Hameed, B. H., Krishni, R. R.,& Sata, S. A. [2009]: A novel agricultural waste adsorbent for the removal of cationic dye from aqueous solution. Journal of Hazardous Materials. 162, p. 305-311.
27. Ashori, A., Hazeh, Y., Azadeh, E., Izadyar, S.,Layeghi, M., and Niaraki, M.,M. [2012]: Potential of canola stalk as biosorbent for the removal of remazol black b reactive dye from aqueous solutions canola stalk for removal of RBB. Journal of wood chemistry and technology. 32, p. 328-341.
28. Hameed, B. H. [2009]: Evaluation of papaya seeds as a novel non-conventional low cost adsorbent for removal of methylene blue. Journal of Hazardous Materials. 162, p. 939-944.
29. Meshkani F, Rezaei M. [2009]: Facile synthesis of nanocrystalline Magnesium oxide with high surface area. Powder Technology. 196(1), p. 8-85.
30. G. F. Huang , Q. T. Wu, J. W. C. Wong, B. B. Nagar. [2005]: Transformation of organic matter during co-composting of pig manure with sawdust, Bioresource Technology. 35, p. 132-137.
31. Srivastava V, Sharama YC, Sillanpaa M. [2015]: Response surface methodology approach for the optimization of adsorption process in the removal of Cr(VI) ions by Cu2(OH)2CO3 nanoparticles. Applied Surface Science. 326, p. 257-70.
32. K.M. Sundaram, J. Curry and M. Landmark, J. Environ. Sci. Health B, [1995]: 30, p. 827-839.
33. Satapathy MK, Das P. [2014]: Optimization of crystal violet dye removal using novel soil-silver nanocomposite as nanoadsorbent using response surface mythology .Journal of Enviromental Chemical Engineering. 2(1), p. 708-14.
34. Lundstedt T, Seifert E, Abramo L. Thelin B, Nystrom A. Pettersen J.[1998]: Experimental design and optimization. Chemometrics and Intelligent Laboratory systems. 42(1-2), p. 3-40.
35. Roosta M., Ghaedi M, Daneshfar A, Saharei R. [2014]: Experimental design based response surface methodology

optimization of ultrasonic assisted adsorption of safaranin O by tin sulfide nanoparticle loaded on activated carbon. Spectrochimica Acta Part A: Molecular and Biomolecular Spectroscopy. 122, p. 223-31.

36. Frendlich H. M. F., Over the adsorption in solution, J. pof Phy. Che. [1906]: 57, p. 385-470.
37. Kannusamy P, Sivalingam, T. [2013]: Synthesis of porous chittosan- polyaniline / ZnO hybrid composite and application for removal of reactive orange 16 dye. Colloids and surface B: Bio interfaces. 108, p. 229-38.
38. Langmuir I. [1916]: The concentration and fundamental properties of solid and liquid, J. Am, chem. Soc. 38 (11), p. 2221-2295.
39. Temkin M. J. and Pyzhev. [1940]: Recent modifications to Langmuir isotherms. Acta physicochimica URss. 12, p. 217-22.
40. Seyed Hassan Sharifi, Hassan Shoja. [2018]: Optimization of process variables by response surface methodology for methylene blue dye removal using spruce sawdust/MgO nanobiocomposite. J. Water Environ Nanotechnol. 3(2), p. 157-172.
41. M. Hema, S. Arivoli. [2007]: Comparative study on the adsorption kinetics and thermodynamics of dyes onto acid activated low cist carbon. International Journal of physical Sciences. 2(1), p. 10-17.
42. Ahmad A. Khatoon A, Mohd-Setapar S-H , Kumar R, Rafatullah M. [2015]: Chemically oxidized pineapple fruit peel for the biosorption of heavy metals from aqueous solution. Desalination and water treatment. 57 (14), p. 6432-42.
43. Yagub MT,Sen TK, Afroze S, Ang HM. [2014]: Fixed-bed dynamic column adsorption study of methylene blue (MB) onto pine cone. Desalination and water treatment. 55(4), p. 1026-39.
44. Yu X, Tong S, Ge M, Wu L, Cao C. [2013]: Adsorption of heavy metal ions from aqueous solution by carboxylated cellulose nanocrystals. Journal of Environmental Sciences. 25(5), p. 933-43.
45. Deniz F . Kepekci RA. [2016]: Dye biosorption onto pistachio by product : A green environmental engineering approach. Journal of Molecular liquids. 219, p.194-200.
46. Oo Cw, Kassim MJ, Pizzi A. [2009]: Characterization and preformabce of Rhizophora apoculata mangrove polyflvonoid tannins in the adsorption of copper (II) and lead (II) . Industrial crops and products. 30 (1), p. 152-61.
47. Nasuha N, Hameed BH, Din ATM. [2010]: Rejected tea as a potential low –cost adsorbent for the removal of methylene blue. Journal of Hazardous Materials. 175(1-3), p. 126-32.

48. Z. Zhang, L. Moghaddam, I. M.O'Hara, W. O. S. Doherty. [2011]: Congo Red adsorption of dyes by ball-milled sugarcane bagasse, Chem. Eng. J. 178, p. 263-274.
49. Bakulina Vm. Tokareva SA, Latysheva EL, Vol' nov II. [1970]: X-ray diffraction study of magnesium superoxide $Mg(O_2)_2$, Journal of Structural Chemistry. 11(1), p. 150-1.
50. Sharifi Pajaie H, Taghizadeh M. [2015]: Optimization of nano-sizwd SAPO-34 synthesis in methanol-to-olefin reaction by response surface methodology. Journal of Industrial and Engineering Chemistry. 24, p. 59-70.
51. Raffiea Baseri J, Palanisamy P N and Sivakumar P. [2012]: comparative studies of the adsorption of direct dye on activated carbon and conducting polymer composite, E-Journal of chemistry. 9(3), p. 1122-1134.

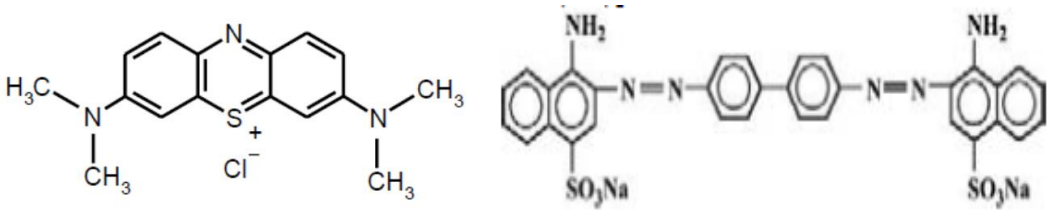

-a- -b-

Figure1. Chemical structure of -a- MB. –b- CR.

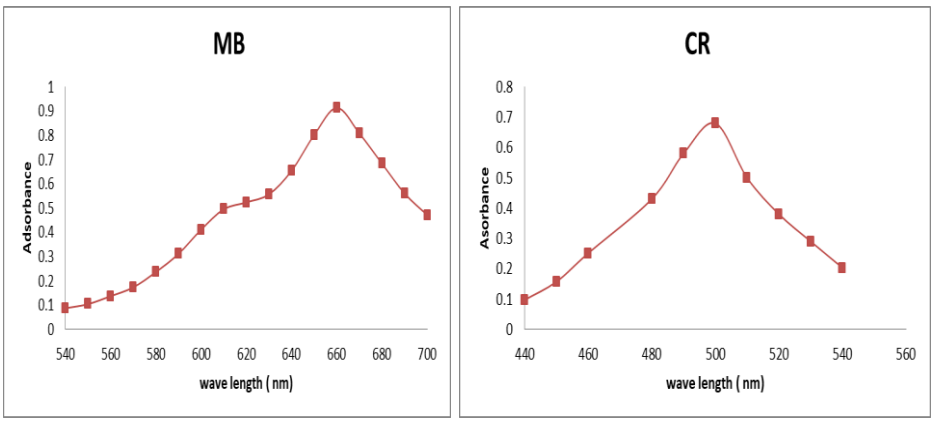

Figure2. The λ_{max} value of (a) MB (b) CR.

Table1. The physico-chemical properties of each adsorbent that used.

no	Types of adsor	Moister conten	pH	CEC µS	TDS mg/L
1	SD/MgO	-	8.9	1238.48	515.13
2	Sawdust	10.2	5.26	216.48	100.13

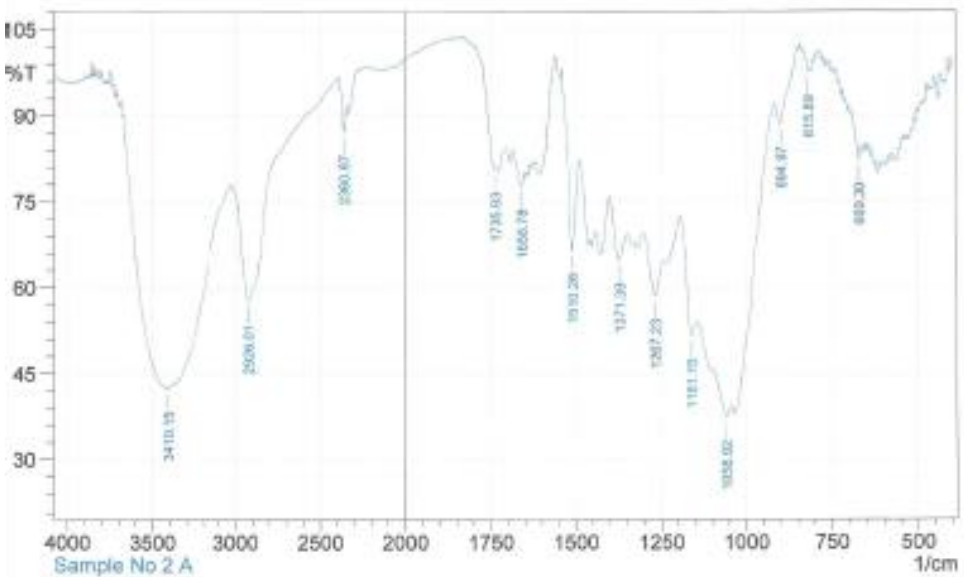

-a-

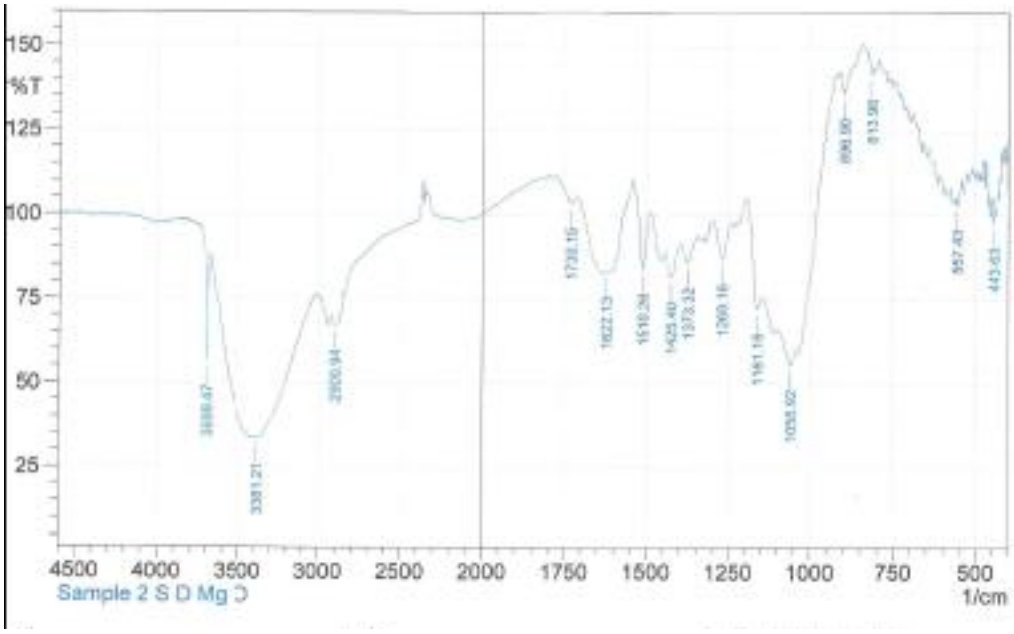

-b-

Figure3. FTIR Spectrum of (a) SD before adsorption (b) SD/MgO before adsorption.

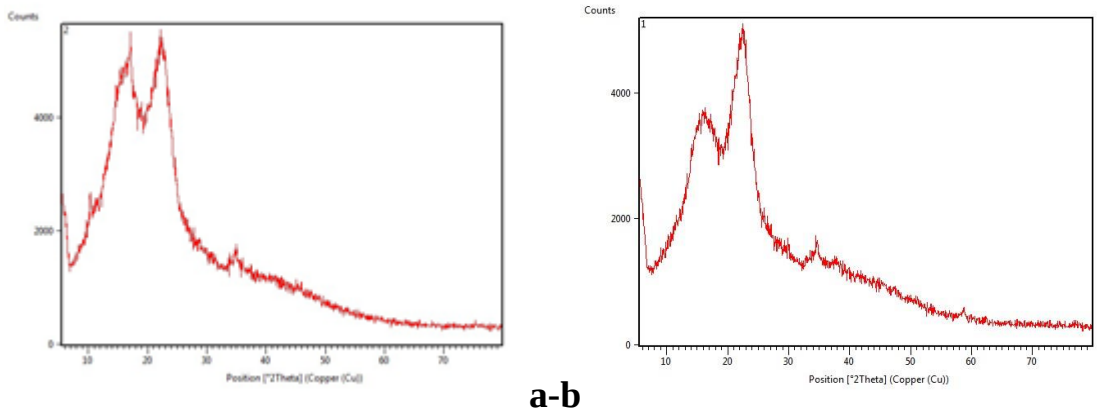

a-b

Figure4. XRD diffractogram of (a) SD (b) SD/MgO.

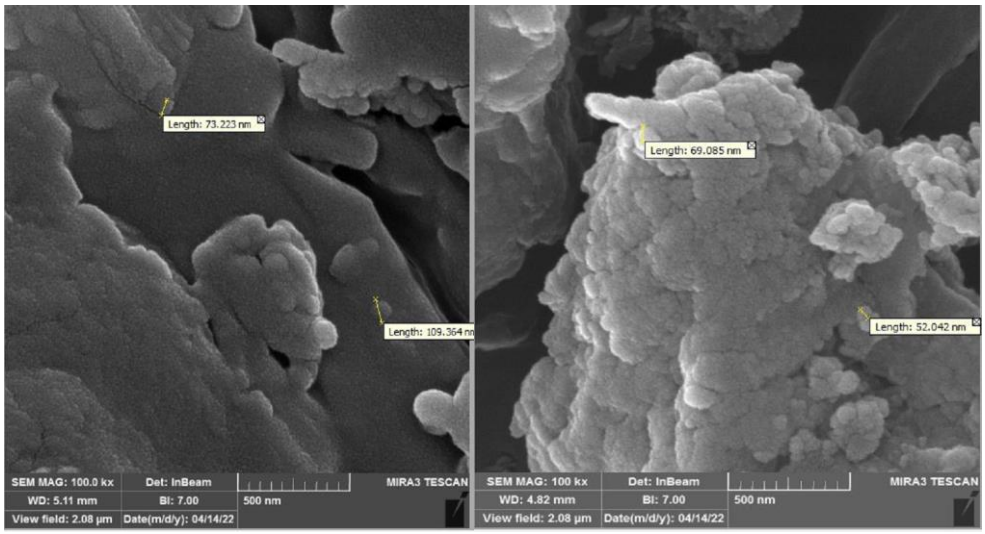

a-b-

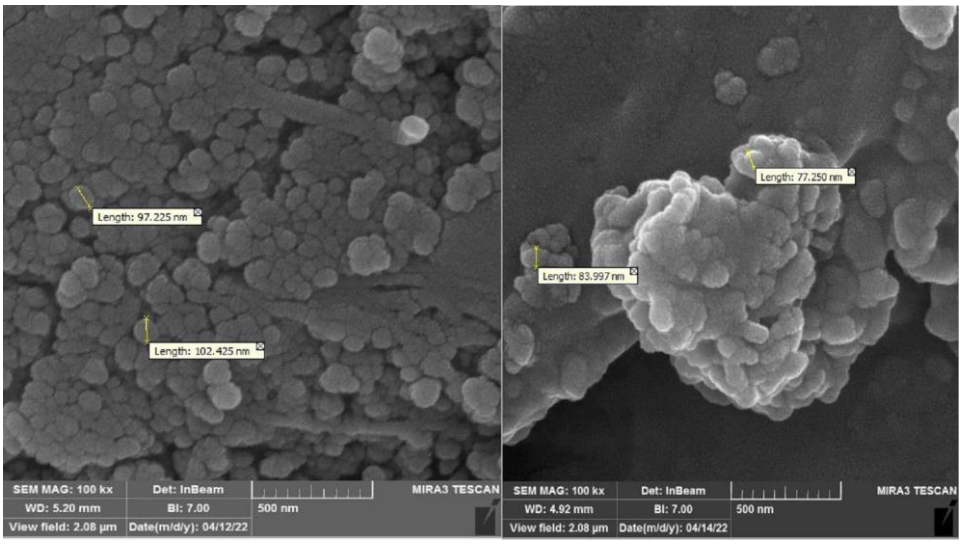

-c-d-

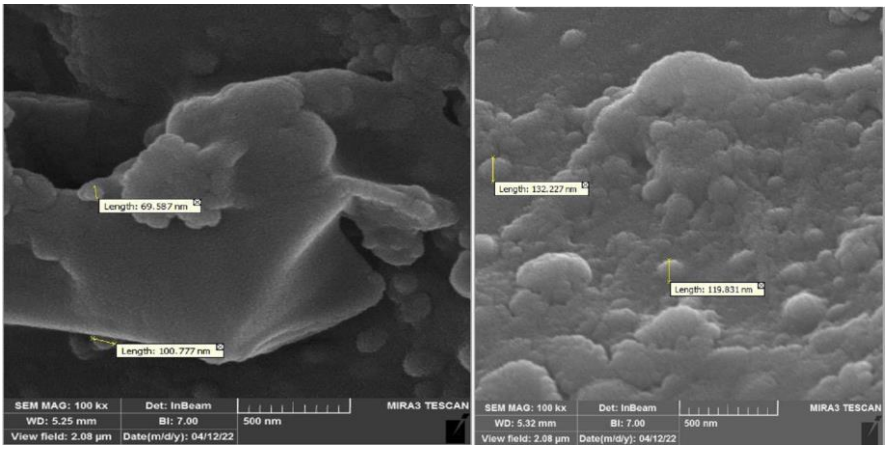

e-f-

Figure5. SEM micrographs for a-SD, b-SD/MgO before adsorption,-c-SD–MB,-d-SD/MgO-MB, -e-SD–CR, and, -f- SD/MgO-CR after adsorption.

Table2. FTIR spectra band before and after adsorption process.

Assignment	Band Position in cm $^{-1}$					
	SD			SD/MgO		
	Before adsor	After adsor MB	After adsor CR	Before adsor	After adso MB	After adso CR
O-H Stre.	3410.15	3392.79	3429.43	3699.43	3404.36	3429.43
C-H Stre. alkyl group	2926.01	2889.37	----------	2900.94	2885.51	2368.59

C═O Stre .of anhydride	1658.78	1647.21	1637.56	1730.15	1600.92	1653.00
C═C aromatic ring	1510.26	1508.33	1508.33	1510.26	1508.33	1508.33
C-O Stre	1267.23	1271.09	----------	1269	1269.12	1273.02
C-N Stre. alifatic 1^{O} amine	1371.39	1373.32	----------	1373.32	1384.89	---------
C-X Stre. carbon halogen group	669.30	599.86	507.28	557.43	669.30	447.49

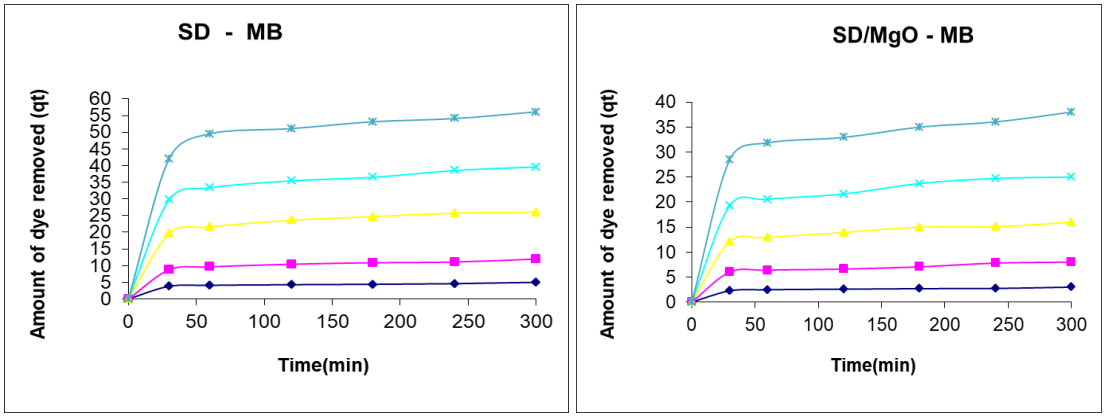

a-b

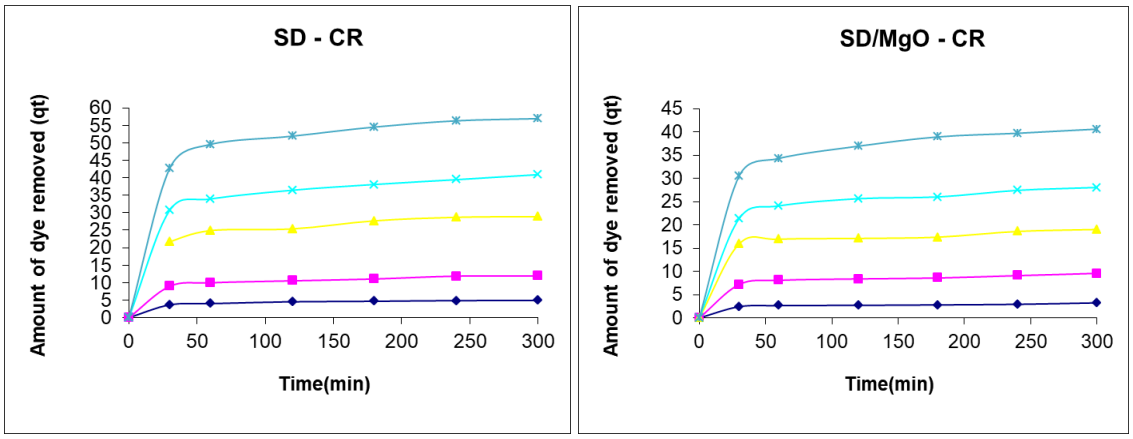

c-d

Figure6. Effect of Agitation Time at 25°C for (a) SD (b) SD/MgO for MB, and (c) SD (d) SD/MgO For CR.

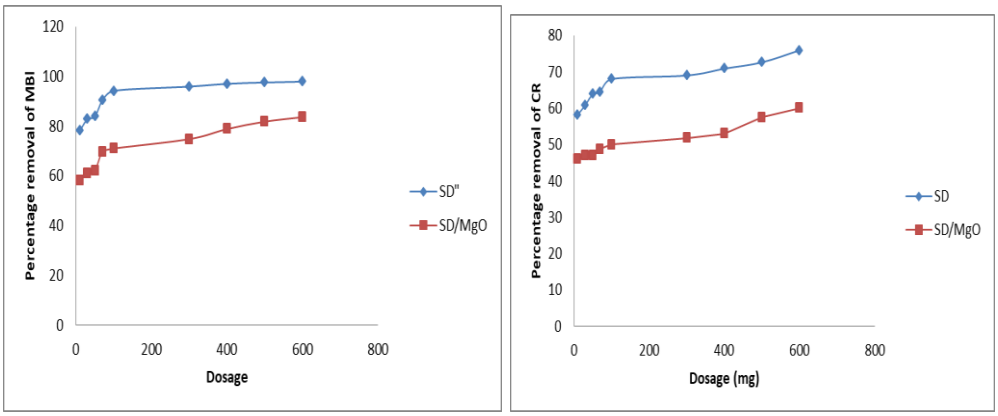

a-b

Figure7. Effect of adsorbent dosage at 25°C for (a) MB on SD and SD/MgO (b) CR onSD and SD/MgO.

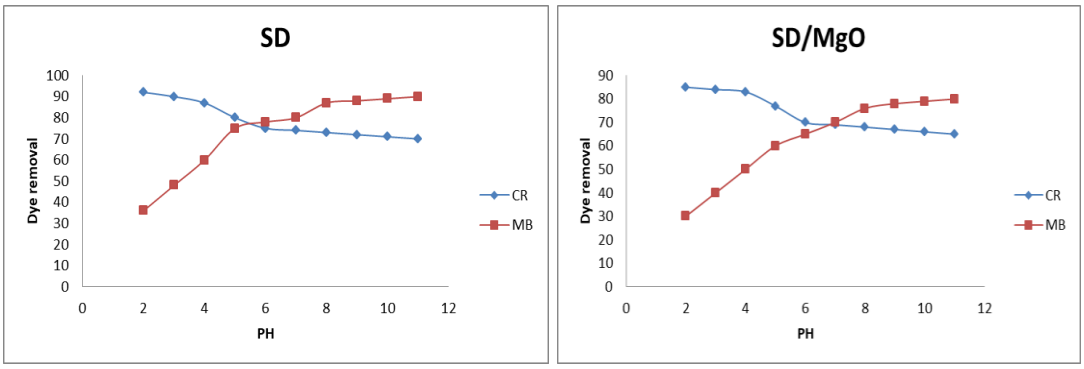

a-b

Figure8. Effect of pH at 25°C for (a) MB and CR on SD (b) MB and CR on SD/MgO.

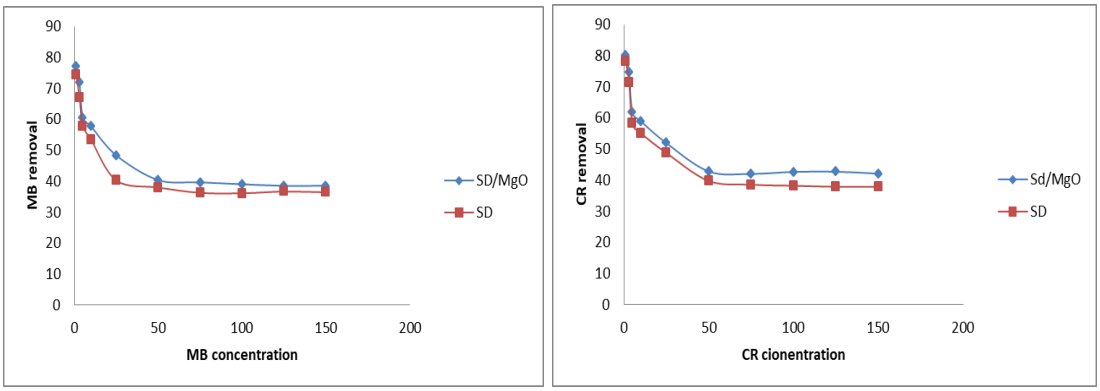

a-b

Figure9. Effect of concentration of dyes at 25°C for (a) MB on SD and SD/MgO for MB, (b) CR on SD and SD/MgO.

Table3. Pseudo first and second order rate constants and intra particle diffusion for adsorption of MB & CR on SD & SD/Mgo at 298K.

Adsorbent	adsorbate	Conc.	Pseudo first order rate		Pseudo second order rate		Intra particle diffusion	
			K_1 (min^{-1})	R^2	K_2 (g µg $^{-1}min^{-1}$)	R^2	K_{id} (mg/ (g min ^{½})	R^2
SD	MB	10	0.022	0.970	0.008	0.999	0.088	0.941
		25	0.024	0.984	0.003	0.999	0.246	0.971
		50	0.023	0.993	0.005	0.998	0.547	0.969
		75	0.025	0.946	0.002	0.998	0.777	0.900
		100	0.026	0.939	0.006	0.999	1.017	0.876
	CR	10	0.020	0.979	0.013	0.999	0.121	0.971
		25	0.021	0.830	0.004	0.998	0.267	0.975
		50	0.020	0.915	0.027	0.997	0.646	0.935
		75	0.014	0.993	0.003	0.999	0.843	0.976
		100	0.019	0.961	0.005	0.999	1.246	0.920
SD/MgO	MB	10	0.023	0.955	0.005	0.999	0.053	0.943
		25	0.023	0.818	0.002	0.998	0.169	0.949
		50	0.023	0.956	0.001	0.999	0.320	0.983
		75	0.023	0.963	0.001	0.999	0.509	0.979
		100	0.024	0.977	0.001	0.999	0.725	0.969
	CR	10	0.016	0.950	0.006	0.999	0.045	0.939
		25	0.018	0.930	0.002	0.999	0.167	0.918
		50	0.017	0.849	0.001	0.999	0.222	0.871
		75	0.020	0.943	0.001	0.999	0.548	0.925
		100	0.020	0.996	0.001	0.999	0.901	0.955

Table4. Pseudo first and second order rate constants and intra particle diffusion for adsorption of MB & CR on SD & SD/Mgo at 308K.

Adsorbent	adsorbat	Conc.	Pseudo first order rate		Pseudo second order rate		Intra particle diffusion	
			K_1 (min^{-1})	R^2	K_2 (g $\mu g^{-1} min^{-1}$)	R^2	K_{id} (mg/ (g $min^{½}$)	R^2
SD	MB	10	0.025	0.987	0.006	0.999	0.088	0.890
		25	0.025	0.968	0.002	0.999	0.193	0.940
		50	0.027	0.863	0.001	0.998	0.474	0.960
		75	0.026	0.999	0.001	0.999	0.725	0.970
		100	0.025	0.947	0.001	0.999	0.977	0.979
	CR	10	0.015	0.923	0.006	0.998	0.097	0.878
		25	0.018	0.817	0.002	0.997	0.243	0.974
		50	0.021	0.943	0.002	0.999	0.584	0.993
		75	0.022	0.969	0.002	0.999	0.913	0.991
		100	0.020	0.948	0.001	0.999	1.090	0.959
SD/MgO	MB	10	0.021	0.961	0.007	0.999	0.039	0.948
		25	0.028	0.946	0.002	0.999	0.092	0.824
		50	0.021	0.888	0.001	0.999	0.198	0.880
		75	0.024	0.9842	0.001	0.999	0.340	0.987
		100	0.026	0.927	0.001	0.999	0.418	0.843
	CR	10	0.014	0.962	0.008	0.999	0.028	0.957
		25	0.017	0.980	0.003	0.999	0.116	0.975
		50	0.018	0.916	0.002	0.999	0.275	0.980
		75	0.016	0.855	0.001	0.999	0.324	0.890
		100	0.021	0.897	0.001	0.999	0.557	0.899

Table 5:Pseudo first and second order rate constants and intra particle diffusion for adsorption of MB & CR on SD & SD/Mgo at 318K.

Adsorbent	adsorbat	Conc.	Pseudo first order rate		Pseudo second order rate		Intra particle diffusion	
			K_1 (min^{-1})	R^2	K_2 (g $\mu g^{-1} min^{-1}$)	R^2	K_{id} (mg/ (g $min^{½}$))	R^2
SD	MB	10	0.024	0.972	0.004	0.999	0.071	0.978
		25	0.026	0.941	0.002	0.999	0.170	0.910
		50	0.024	0.95	0.001	0.999	0.395	0.992
		75	0.024	0.987	0.001	0.998	0.612	0.988
		100	0.026	0.957	0.001	0.997	0.761	0.925
	CR	10	0.019	0.958	0.004	0.999	0.098	0.952
		25	0.022	0.666	0.002	0.999	0.209	0.908
		50	0.018	0.834	0.001	0.999	0.275	0.822
		75	0.017	0.934	0.001	0.999	0.541	0.908
		100	0.022	0.981	0.001	0.999	1.088	0.946
SD/MgO	MB	10	0.015	0.714	0.011	0.999	0.013	0.763
		25	0.017	0.957	0.004	0.999	0.062	0.971
		50	0.023	0.823	0.002	0.999	0.106	0.716
		75	0.021	0.940	0.001	0.999	0.106	0.885
		100	0.029	0.935	0.001	0.999	0.318	0.716
	CR	10	0.029	0.754	0.008	0.999	0.035	0.792
		25	0.020	0.869	0.003	0.999	0.092	0.990
		50	0.019	0.851	0.002	0.999	0.184	0.987
		75	0.016	0.941	0.001	0.999	0.241	0.962
		100	0.018	0.942	0.001	0.999	0.398	0.985

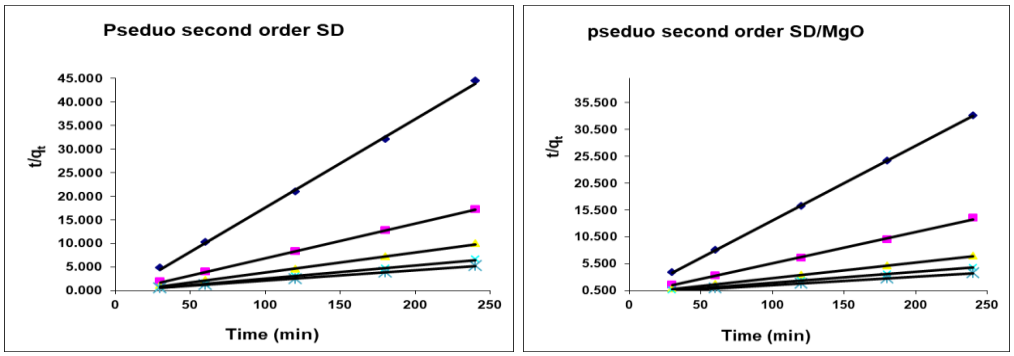

a-b-MB

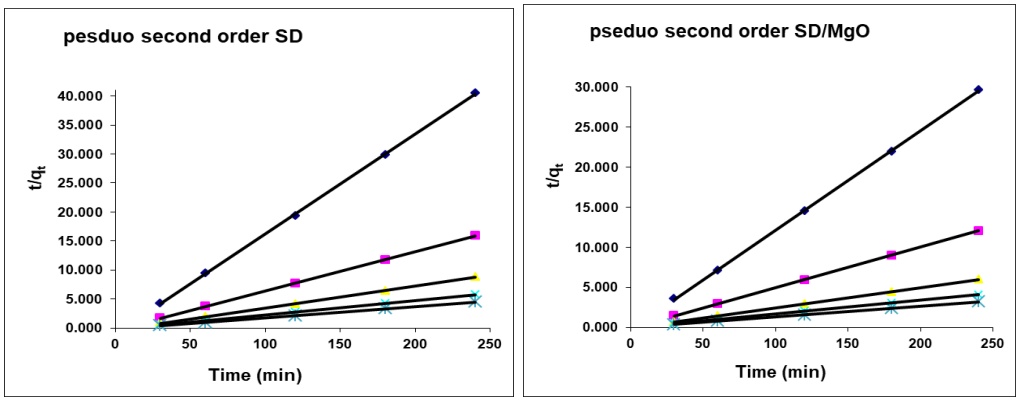

c-d-MB

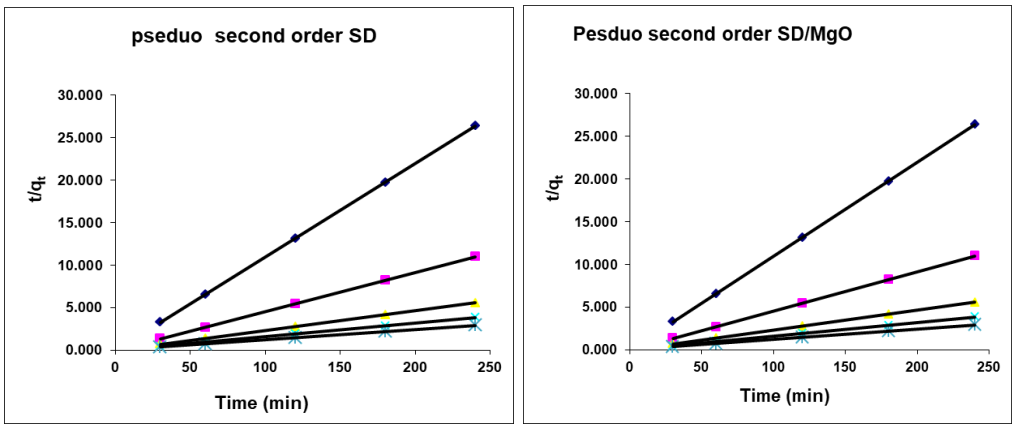

e-f-MB

Figure10. Pseudo second order rate constants for adsorption of MB on SD & SD/Mgo for concentration (♦ 10, ■ 25, ▲ 50, x75, * 100) ppm, a-b at 298K, c-d at 308K and e-f at 318K.

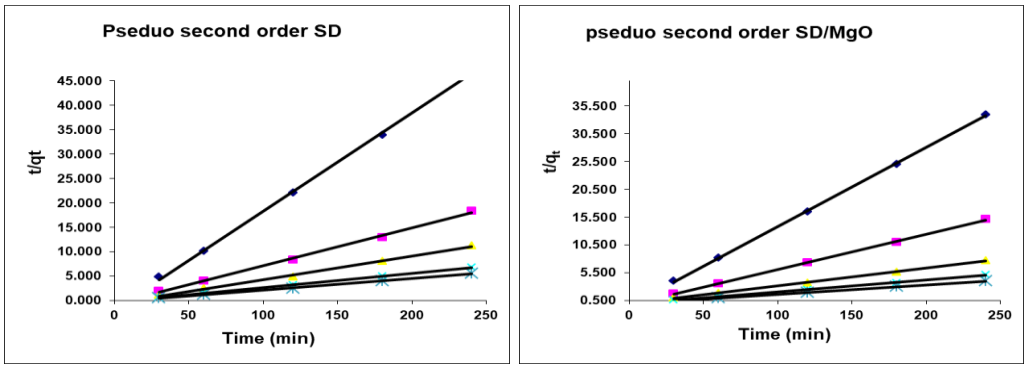

a-b-CR

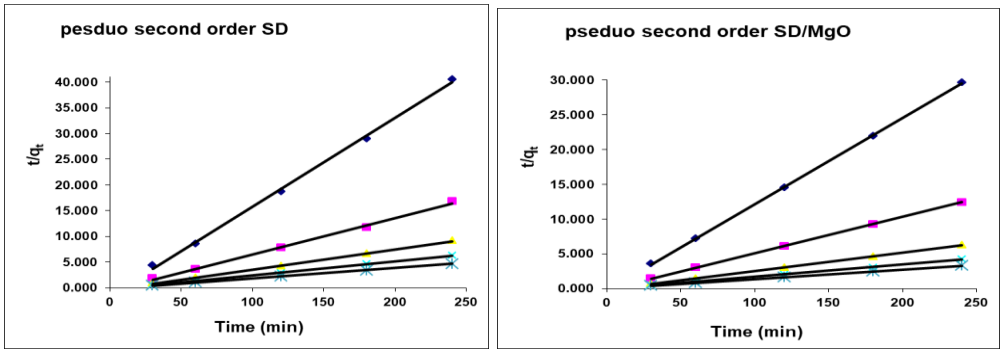

c-d-CR

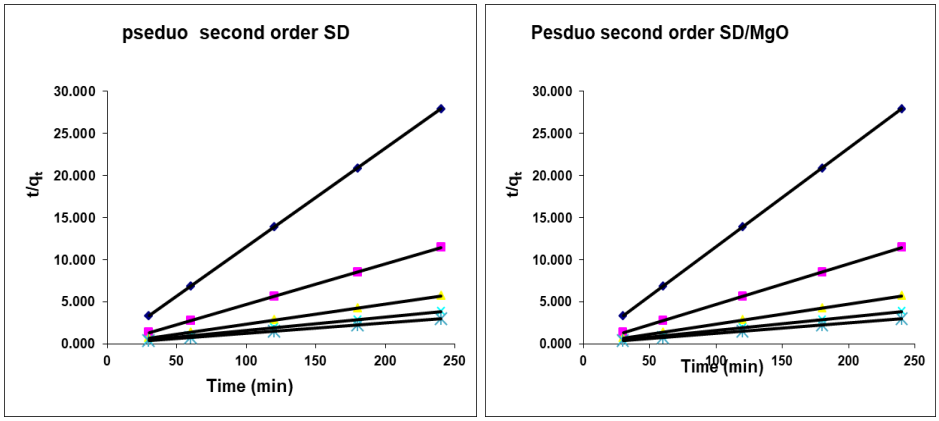

e-f-CR

Figure11. Pseudo second order rate constants for adsorption of CR on SD & SD/Mgo for concentration (♦ 10, ■ 25, ▲ 50, x75, * 100) ppm , a-b at 298K, c-d at 308K and e-f at 318K, a-b at 298K, c-d at 308K and e-f at 318K.

Table6. Adsorption Isotherm parameters for the models Freundlich, Langmuir and Temkine for MB and CR at 298.15 K.

Adsorption Models	Parameter	SD		SD/MgO	
		MB	CR	MB	CR
Freundlich	K_F(mL/g)	31.88	44.05	276.3	57.74
	S.E	0.812	0.816	0.127	0.0935
	n_F	1.119	1.256	1.145	1.119
	R^2	0.999	0.892	0.873	0.944
Langmuir. coffi.	K_L (ml/g)	0.008	0.012	0.012	0.009
	S.E	0.201	0.207	0.133	0.14
	C_m(µg/g)	2500	2500	5000	5000
	R^2	0.983	0.749	0.945	0.856
Temkin.coffi.	α (A) (l/g)	6.964	8.63	34.294	36.61
	β (B) (J/mg)	441.02	2031	2172	36.61
	R^2	0.963	0.908	0.949	0.890

Table7. Adsorption Isotherm parameters for the models Freundlich, Langmuir and Temkine for MB and CR at 308.15 K.

Adsorption Models	Parameter	SD		SD/MgO	
		MB	CR	MB	CR
Freundlich	K_F(mL/g)	51.333	46.98	427.6	99.13
	S.E	0.881	0.0835	0.139	0.107
	n_F	1.201	1.251	1.105	1.119
	R^2	0.999	0.950	0.994	0.993
Langmuir. coffi.	K_L (ml/g)	0.073	0.007	0.010	0.0090
	S.E	0.175	0.182	0.198	0.969
	C_m(µg/g)	5000	5000	10000	10000
	R^2	0.996	0.829	0.889	0.837
Temkin. coffi.	α (A) (l/g)	9.033	13.18	47.909	33.21
	β (B) (J/mg)	498.58	472.84	2644.4	2524
	R^2	0.963	0.956	0.950	0.928

Table8. Adsorption Isotherm parameters for the models Freundlich, Langmuir and Temkine for MB and CR at 318.15 K.

Adsorption Models	Parameter	SD		SD/MgO	
		MB	CR	MB	CR
Freundlich	K_F(mL/g)	67.19	46.63	864.6	170.69
	S.E	0.948	0.090	0.152	0.118
	n_F	1.195	1.115	1.272	2.232
	R^2	0.999	0.989	0.997	0.993
Langmuir. coffi.	K_L (ml/g)	0.004	0.008	0.005	0.032
	S.E	0.14	0.164	0.16	0.688
	C_m(µg/g)	10000	5000	5000	5000
	R^2	0.906	0.723	0.940	0.884
Temkin. coffi.	α (A) (l/g)	28.332	33.86	138.1	36.11
	β (B) (J/mg)	516.3	484.67	2518	2669
	R^2	0.927	0.939	0.928	0.934

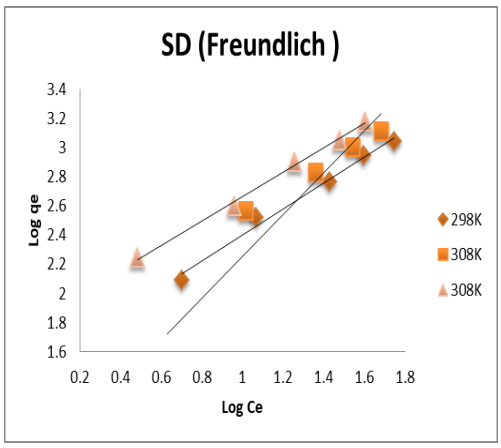

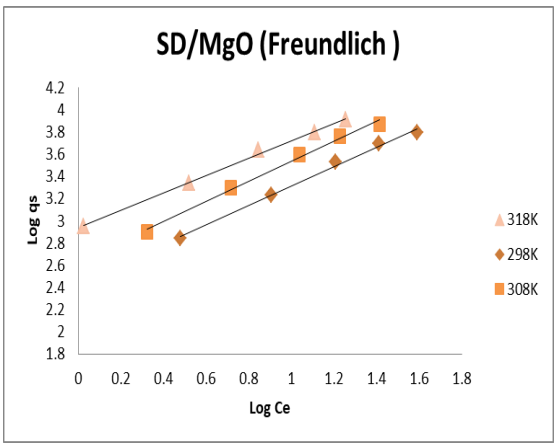

a-b - MB

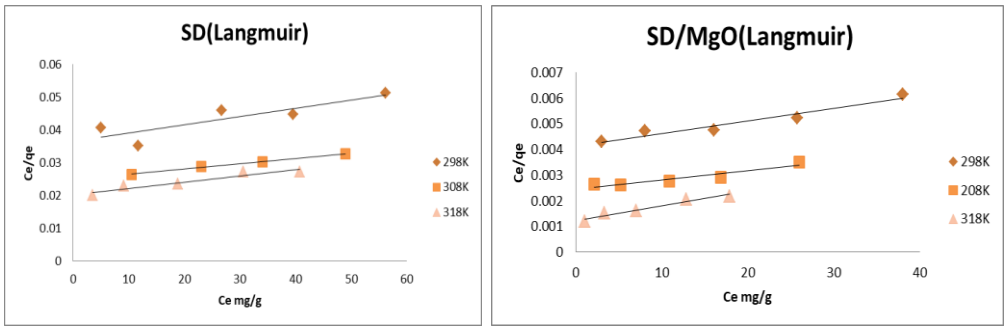

c-d -MB

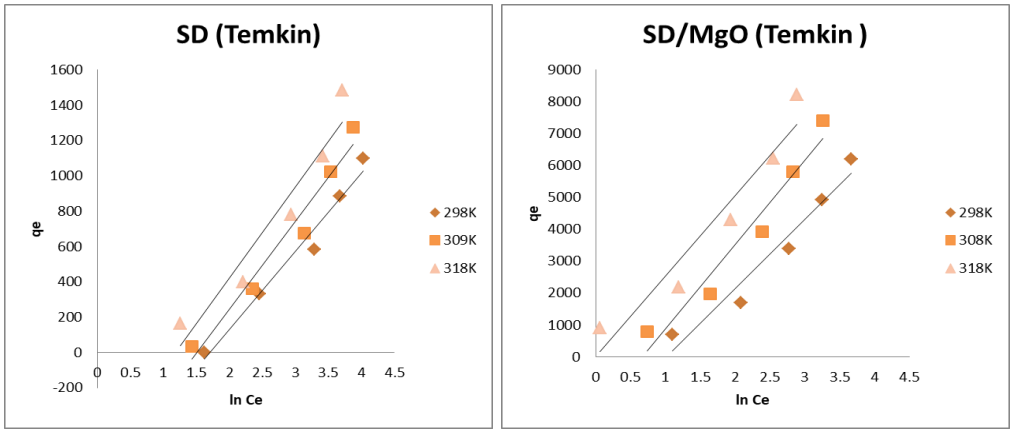

e-f - MB

Figure12. Adsorption Isotherm models for Freundlich, Langmuir and Temkine for MB at 298, 308 and 318 K of MB & CR on SD & SD/Mgo.

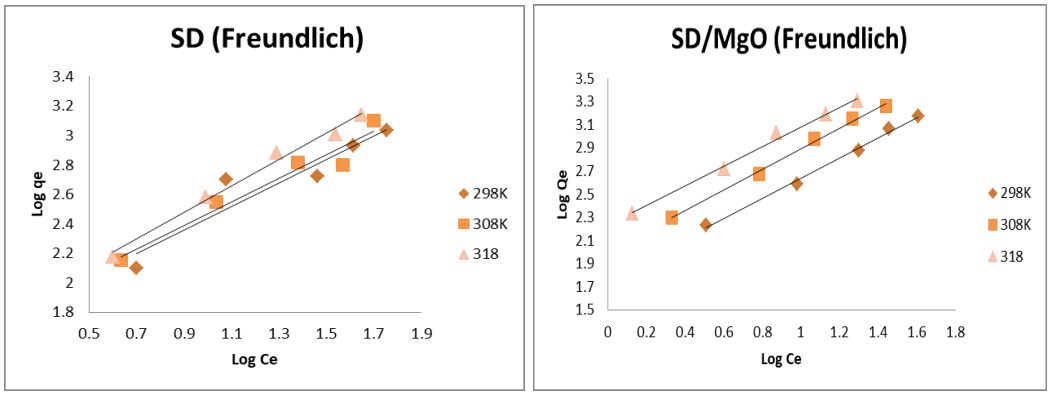

a-b-CR

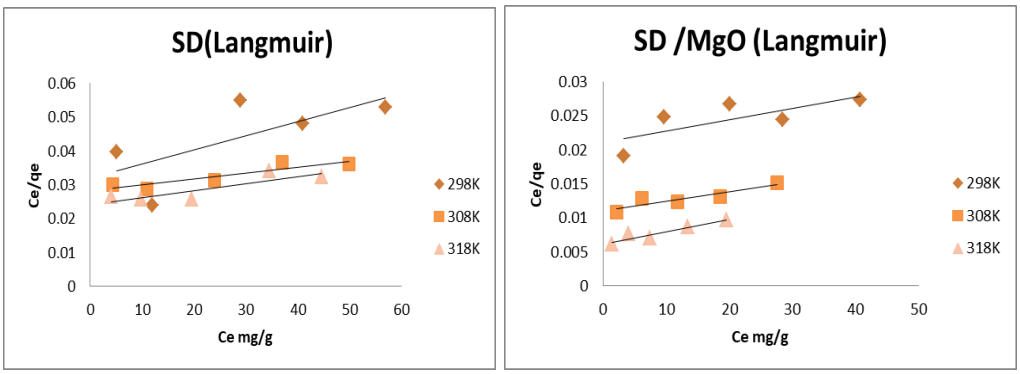

c-d-CR

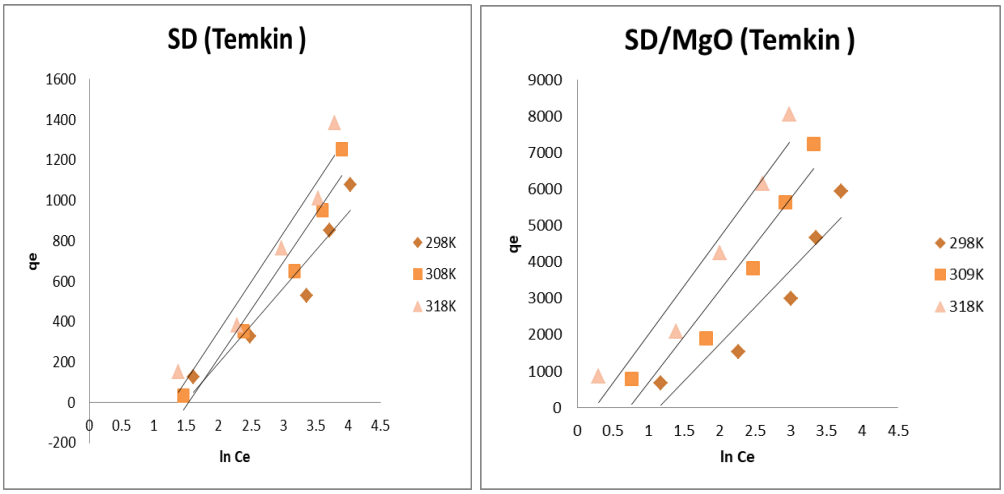

e-f-CR

Figure13. Adsorption Isotherm models for Freundlich, Langmuir and Temkine for CR at 298, 308 and 318 K of MB & CR on SD & SD/Mgo.

Table9. Free energy change, standard entropy change and standard enthalpy change for adsorption of MB and CR on the SD and SD/MgO at three temperatures.

Temp (K)	Parameter	SD		SD/MgO	
		MB	CR	MB	CR
289K	K_o	433	443.3	14371	8583
	ΔG (kJ/mol	-14794	-14853	-22536	-21322
309K	K_o	716	637	26012	26035
	ΔG (kJ/mol	-16841	-16543	-26046	-26048
318K	K_o	3050	1664	29166	28618
	ΔG (kJ/mol	-21222	-19618	-27194	-27145
ΔH (kJ/mol)		76.576	51.883	28.104	47.902
ΔS (kJ/mol. K)		0.306	0.224	0.175	0.237
Ea (kJ/mol)		79.06	54.36	30.75	50.46
R^2		0.917	0.927	0.880	0.823

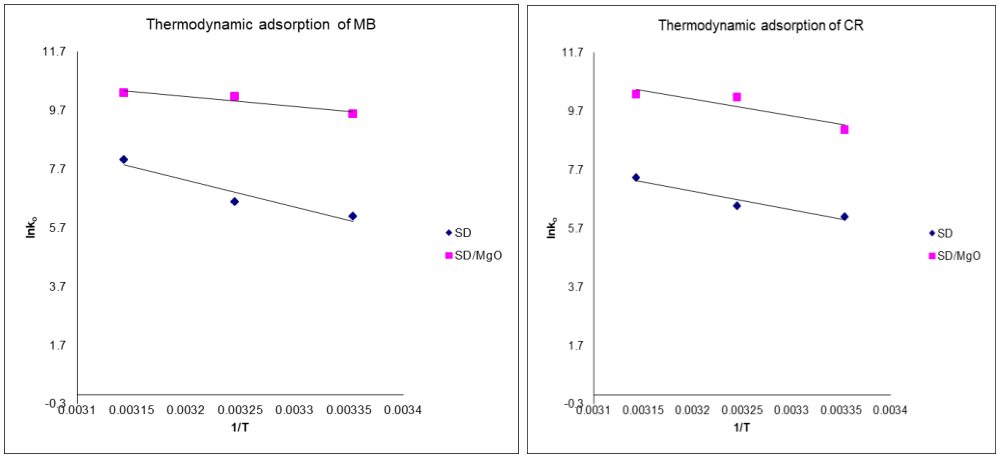

Figure13. Variation of ln K_o with 1/T for adsorption of MB and CR on SD and SD/MgO.